Vietnam Journal of Science and Technology ***56*** *(4) (2018) 515-530*

DOI: 10.15625/2525-2518/56/4/10978

CONTINUOUS ELEMENT FORMULATIONS FOR COMPOSITE RING-STIFFENED CYLINDRICAL SHELLS

Le Thi Bich Nam[1,*], Nguyen Manh Cuong[1], Tran Ich Thinh[1], Tran Thanh Dat[2], Vu Dinh Trung[2]

[1] *School of Mechanical Engineering, HUST, 1 Dai Co Viet, Ha Noi*

[2]*Department of Space and Applications, HUST, 1 Dai Co Viet, Ha Noi*

[*]Email: *bichnamvl@gmail.com*

Received: 18 December 2017; Accepted for publication: 10 June 2018

Abstract. This article studies the free vibration of composite ring-stiffened cylindrical shells by the continuous element method (CEM). The dynamic stiffness matrix (DSM) of the studied structure has been constructed based on the analytical solutions of the governing equations of motion for composite cylindrical shells and annular plates. By applying the assembly procedure of the continuous elements method, natural frequencies and harmonic responses of composite ring-stiffened cylindrical shells are determined. In addition, the proposed model allows to exactly extract ring-stiffener vibration modes. Numerical examples confirm advantages of the proposed model: high precision solution even in medium and high frequencies, saving in calculating time and volume of data storage.

Keywords: continuous element method, laminated composite cylindrical shell, ring stiffener shell.

Classification numbers: 5.4.2; 5.4.3; 5.4.5.

1. INTRODUCTION

Ring-stiffened laminated cylindrical shells have been widely used in applications such as tankers, pipelines, aircrafts, and submarines. Ring stiffeners may be used to connect parts of a shell together to make a longer cylindrical shell or to reinforce a shell's structure. Therefore, the requirement of technical information about dynamic behaviors of such complex structures is of great importance. Studies on ring-stiffened isotropic cylindrical shells have been mentioned by various researchers [1-3]. Najafi and Warburton [4] investigated the natural frequency and mode shape of a thin cylindrical shell with ring stiffeners by using the finite element method (FEM). Mustafa and Ali [5] gave the information about natural frequencies of a stiffened cylindrical shell by using the Rayleigh–Ritz procedure. Furthermore, the free vibration analysis of the rotating cylindrical shell which simply supported by circumferential stiffeners, rings with non-uniform stiffeners eccentricity and non-uniform stiffeners spacing distribution was demonstrated by Jafari and Bagheri [6]. Qu et al. [7] presented a modified vibrational approach for the vibration of a ring-stiffened conical-cylindrical-sphere combined shell. Recently, the vibration of

laminated cylindrical shells with ring stiffeners also has been investigated. Kim and Lee [8] used a theoretical method to examine the effects of ring stiffeners on vibration characteristics and transient responses of the ring-stiffened composite cylindrical shells which subjected to the step pulse loading. The Love's thin shell theory was combined with the discrete stiffener theory to consider the effect of ring stiffeners. Here the ring stiffeners were made of laminated composite material and had a uniform rectangular cross-section. The Rayleigh-Ritz procedure was applied to obtain the frequency equations. Zhao et al. [9] analyzed the free vibration of simply supported rotating cross-ply laminated cylindrical shells with axial and circumferential stiffeners, using an energy approach. The effects of these stiffeners were evaluated by two methods: stiffeners were treated as discrete elements and the properties of the stiffeners were averaged over the shell surface by the smearing method. Especially, an interesting vibration analysis of ring-stiffened cross-ply laminated cylindrical shells was done by Wang and Lin [10]. Two different materials were used for cylindrical shells and rings with clamped-clamped boundary condition and the effects of ring depth, ring width and lamination scheme on natural frequencies of joined ring stiffened cylindrical shells were considered. Kouchakzadeh and Shakouri [11] considered the free vibration analysis of joined cross-ply laminated conical shells by using the Donnell thin shell theory. Nevertheless, all the references mentioned above focused on the Rayleigh–Ritz method, experiment tests, the finite element method (FEM) and the classical thin shell theory. It is necessary to note that analytical methods meet many difficulties in constructing the system of equations to solve for complex structures. In addition, although the FEM can provide good results in certain low frequencies, it will be less efficient for the high frequency range because of the discretization of the domain which can accumulate errors and affects the precision of solutions.

The Dynamic Stiffness Method (DSM) or the Continuous Element Method (CEM) [12-16] has been developed in order to overcome these difficulties of the FEM in dynamic problems. The CEM is based on the exact closed form solution of the governing differential equations of motion which lead to the dynamic stiffness matrix relating a state vector of loads to the corresponding state vector of displacements at the edges of the structure [12, 13]. By using the CE model, one or three continuous elements are enough to compute any range of frequencies with desired accuracy. In addition, continuous elements can also be assembled together in order to model more complex structures by using the similar principle of assembly in the FEM. The use of minimum of continuous elements allows a fast acquisition of harmonic response thus it reduces the computing time compared to the FEM. The disadvantage of the CEM is the lack of a large library of continuous elements covering all kinds of structures as in the FEM. Therefore, new dynamic stiffness formulations for building new isotropic and composite continuous elements are in strong development. Recent formulations have concerned all kinds of structural elements such as isotropic and composite shells [12-13], and stiffened isotropic cylindrical shells [14]. Recently, Casimir et al. [15], Thinh and Nguyen [16] considered the dynamic response of a cross-ply laminated composite shell with the dynamic stiffness method.

Despite of abundant continuous elements constructed for composite plates and shells, the dynamic stiffness formulations for composite stiffened cylindrical shells have never been mentioned before. The purpose of this paper is presenting a continuous element for vibration analysis of thick cross-ply laminated composite ring-stiffened cylindrical shells. Numerous numerical tests and comparisons will be conducted in order to validate our model as well as to demonstrate main advantages of the CEM.

2. THEORETICAL FORMULATIONS

2.1. The ring-stiffened cylindrical shells

The ring-stiffened cylindrical shell under the consideration as shown in Figure 1 has a constant thickness h, radius R and lengths L_1, L_2. The reference surface is taken at the middle surface of the shell where an orthogonal coordinate system (s,θ,z) is determined as in Figure 1. The s coordinate is taken in the axial direction where θ and z are, respectively in the circumferential and the radial directions of the shell. The displacements of the shell in the s, θ and z directions are denoted by u, v and w respectively. Specially, the ring of ring-stiffened shells is accepted to be isotropic or composite material, with width c_r and thickness b_r.

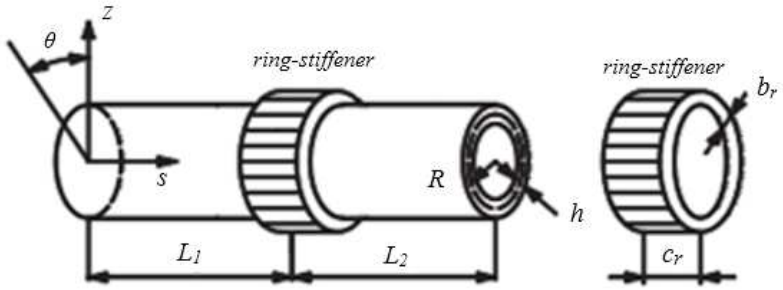

Figure 1. A laminated stiffened cylindrical shell with a circumferential outer ring-stiffener.

2.2. Theory of laminated composite cylindrical, conical shells and rings

2.2.1. Lamina constitutive relations

Consider a laminate composite shell of total thickness h composed of N orthotropic layers, the principal material coordinates $\left(x_1^i, x_2^i, x_3^i\right)$ of the i^{th} layer oriented at an angle θ to the laminate coordinate x_1. The plane stress-reduced stiffness is calculated as:

$$Q_{11}=\frac{E_1}{1-\upsilon_{12}\upsilon_{21}},\ Q_{12}=\frac{\upsilon_{12}E_2}{1-\upsilon_{12}\upsilon_{21}},\ Q_{22}=\frac{E_2}{1-\upsilon_{12}\upsilon_{21}},$$
$$Q_{66}=G_{12},\ Q_{44}=G_{23},\ Q_{55}=G_{13} \tag{1}$$

here: E_i, G_{ij}, υ_{12}, υ_{21} are elastic constants of the k[th] layer.

And the laminate stiffness coefficients (A_{ij}, B_{ij}, D_{ij}) are defined by [17]:

$$\begin{aligned}
A_{ij} &= \sum_{k=1}^{N}\overline{Q}_{ij}^{k}(z_{k+1}-z_k)\ (i,j=1,2,6)\\
A_{ij} &= \sum_{k=1}^{N}\overline{Q}_{ij}^{k}(z_{k+1}-z_k)\ (i,j=4,5)\\
B_{ij} &= \frac{1}{2}\sum_{k=1}^{N}\overline{Q}_{ij}^{k}(z_{k+1}^2-z_k^2)\\
D_{ij} &= \frac{1}{3}\sum_{k=1}^{N}\overline{Q}_{ij}^{k}(z_{k+1}^3-z_k^3)\ (i,j=1,2,6)
\end{aligned} \tag{2}$$

where z_{k-1} and z_k are the boundaries of the k^{th} layer.

2.2.2. Kinematics of composite shells of the revolution

Consider a typical shell of the revolution was represented by a conical shell, as shown in Figure 2. R_1 and R_2 are radius at small and large edges of the cone respectively, α is a semi vertex angle of the cone, L is the length along its generator. The cone's radius at any point along its length is calculated by:

$$R(s) = R_1 + s\sin\alpha \tag{3}$$

it is noteworthy to remark that if $\alpha \neq 0$ the above equations will represent composite conical shells, while $\alpha \to 0$ these formulations can be used for composite cylindrical shells and the case $\alpha \to \pi/2$ corresponds to ring stiffeners.

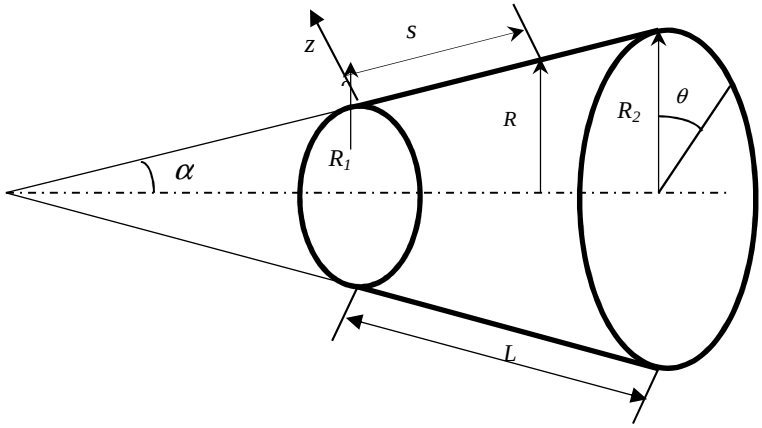

Figure 2. Geometry and coordinate system of a conical shell.

2.2.3. Equations of motion

The equations of motion using the first-order shear deformation shell theory (FSDT) for cross-ply composite circular conical shells are expressed by [17]:

$$\begin{aligned}
&\frac{\partial N_S}{\partial s} + \frac{\sin\alpha}{R}\left(N_S - N_\theta\right) + \frac{1}{R}\frac{\partial N_{S\theta}}{\partial \theta} = I_0\ddot{u}_0 + I_1\ddot{\varphi}_S,\\
&\frac{\partial N_{S\theta}}{\partial s} + \frac{2\sin\alpha}{R}N_{S\theta} + \frac{1}{R}\frac{\partial N_\theta}{\partial \theta} + \frac{\cos\alpha}{R}Q_\theta = I_0\ddot{v}_0 + I_1\ddot{\varphi}_\theta\\
&\frac{\partial M_S}{\partial s} + \frac{2\sin\alpha}{R}\left(M_S - M_\theta\right) + \frac{1}{R}\frac{\partial M_{S\theta}}{\partial \theta} - Q_S = I_1\ddot{u}_0 + I_2\ddot{\varphi}_S,\\
&\frac{\partial M_{S\theta}}{\partial s} + \frac{2\sin\alpha}{R}M_{S\theta} + \frac{1}{R}\frac{\partial M_\theta}{\partial \theta} - Q_\theta = I_1\ddot{v}_0 + I_2\ddot{\varphi}_\theta\\
&\frac{\partial Q_S}{\partial s} + \frac{1}{R}\frac{\partial Q_\theta}{\partial \theta} + \frac{\sin\alpha}{R}Q_S - \frac{\cos\alpha}{R}N_\theta = I_0\ddot{w}_0
\end{aligned} \tag{4}$$

where u_0, v_0, w_0: displacements of a point M_o at the median radius of the shell, φ_S, φ_θ: rotations of the section

$$I_i = \sum_{k=1}^{N}\int_{z_k}^{z_{k+1}}\rho^{(k)}z^i dz \qquad (i = 0,1,2) \tag{5}$$

with $\rho^{(k)}$ is the material mass density of the k^{th} layer.

2.2.4. Force resultants–displacement relationships

The force and moment resultants are written in terms of displacements for the cross-ply conical shell as follows [11]:

$$
\begin{aligned}
N_S &= A_{11}\frac{\partial u_0}{\partial s}+\frac{A_{12}}{R}\left(u_0\sin\alpha+\frac{\partial v_0}{\partial\theta}+w_0\cos\alpha\right)+B_{11}\frac{\partial\varphi_S}{\partial s}+\frac{B_{12}}{R}\left(\varphi_S\sin\alpha+\frac{\partial\varphi_\theta}{\partial\theta}\right)\\
N_\theta &= A_{12}\frac{\partial u_0}{\partial s}+\frac{A_{22}}{R}\left(u_0\sin\alpha+\frac{\partial v_0}{\partial\theta}+w_0\cos\alpha\right)+B_{12}\frac{\partial\varphi_S}{\partial s}+\frac{B_{22}}{R}\left(\varphi_S\sin\alpha+\frac{\partial\varphi_\theta}{\partial\theta}\right)\\
N_{S\theta} &= A_{66}\left(\frac{\partial v_0}{\partial s}+\frac{1}{R}\frac{\partial u_0}{\partial\theta}-\frac{\sin\alpha}{R}v_0\right)+B_{66}\left(\frac{1}{R}\frac{\partial\varphi_S}{\partial\theta}+\frac{\partial\varphi_\theta}{\partial s}-\frac{\sin\alpha}{R}\varphi_\theta\right)\\
M_S &= B_{11}\frac{\partial u_0}{\partial s}+\frac{B_{12}}{R}\left(u_0\sin\alpha+\frac{\partial v_0}{\partial\theta}+\frac{w_0\cos\alpha}{R}\right)+D_{11}\frac{\partial\varphi_S}{\partial s}+\frac{D_{12}}{R}\left(\varphi_S\sin\alpha+\frac{\partial\varphi_\theta}{\partial\theta}\right)\\
M_\theta &= B_{12}\frac{\partial u_0}{\partial s}+\frac{B_{22}}{R}\left(u_0\sin\alpha+\frac{\partial v_0}{\partial\theta}+w_0\cos\alpha\right)+D_{12}\frac{\partial\varphi_S}{\partial s}+\frac{D_{22}}{R}\left(\varphi_S\sin\alpha+\frac{\partial\varphi_\theta}{\partial\theta}\right)\\
M_{S\theta} &= B_{66}\left(\frac{\partial v_0}{\partial s}+\frac{\partial u_0}{R\partial\theta}-\frac{\sin\alpha}{R}v_0\right)+D_{66}\left(\frac{1}{R}\frac{\partial\varphi_S}{\partial\theta}+\frac{\partial\varphi_\theta}{\partial s}-\frac{\sin\alpha}{R}\varphi_\theta\right)\\
Q_\theta &= kA_{44}\left(\frac{-\cos\alpha}{R}v_0+\frac{1}{R}\frac{\partial w_0}{\partial\theta}+\varphi_\theta\right)\qquad Q_S = kA_{55}\left(\frac{\partial w_0}{\partial s}+\varphi_S\right)
\end{aligned}
\tag{6}
$$

where k is the shear correction factor (k = 5/6).

2.3. Dynamic stiffness formulations for thick composite conical, cylindrical shells and annular plates of uniform thickness

2.3.1. State vector of solution

For developing the resolution by the Dynamic Stiffness Method, it is important to choose a state vector of solution. With the examined shells of revolution, the following state vector can be used:

$$\boldsymbol{y}^T = \{u_0,\ v_0,\ w_0,\ \varphi_S,\ \varphi_\theta,\ N_s,\ N_{s\theta},\ Q_x,\ M_s,\ M_{s\theta}\}^T \tag{7}$$

Next, the Fourier series expansion is employed for state variables in the case of symmetric modes as:

$$
\begin{aligned}
&\left\{u_o(s,\theta,t),w_o(s,\theta,t),\varphi_s(s,\theta,t),N_S(s,\theta,t),Q_S(s,\theta,t),M_S(s,\theta,t)\right\}^T=\\
&\sum_{m=1}^{\infty}\left\{u_m(s),w_m(s),\varphi_{sm}(s),N_{S_m}(s),Q_{sm}(s),M_{S_m}(s)\right\}^T\cos m\theta e^{i\omega t}\\
&\left\{v_o(s,\theta,t),\varphi_\theta(s,\theta,t),N_\theta(s,\theta,t),Q_\theta(s,\theta,t),M_\theta(s,\theta,t)\right\}^T=\\
&\sum_{m=1}^{\infty}\left\{v_m(s),\varphi_{\theta m}(s),N_{\theta m}(s),Q_{\theta m}(s),M_{\theta m}(s)\right\}^T\sin m\theta e^{i\omega t}
\end{aligned}
\tag{8}
$$

where m is the number of circumferential wave.

By substituting (8) in equations (4) and (6), a system of ordinary differential equations in the s-coordinate for the m^{th} circumferential mode can be expressed as follows:

$$\frac{du_m}{ds} = \zeta_4 \sin\alpha u_m + m\zeta_4 v_m + \zeta_4 \cos\alpha w_m + \zeta_5 \sin\alpha\varphi_{sm} + m\zeta_5\varphi_{\theta m} + \frac{D_{11}}{\zeta_1} N_{Sm} - \frac{B_{11}}{\zeta_1} M_{sm}$$

$$\frac{dv_m}{ds} = \frac{m}{R} u_m - \frac{\sin\alpha}{R} v_m - \frac{D_{66}}{\zeta_{10}} N_{S\theta m} + \frac{B_{66}}{\zeta_{10}} M_{S\theta m}$$

$$\frac{dw_m}{ds} = -\varphi_{Sm} + \frac{1}{kA_{55}} Q_{Sm}$$

$$\frac{d\varphi_{Sm}}{ds} = \zeta_2 \sin\alpha u_m + m\zeta_2 v_m + \zeta_2 \cos\alpha w_m + \zeta_3 \sin\alpha\varphi_{sm} + m\zeta_3\varphi_{\theta m} - \frac{B_{11}}{\zeta_1} N_{Sm} + \frac{A_{11}}{\zeta_1} M_{Sm}$$

$$\frac{d\varphi_{\theta m}}{ds} = \frac{m}{R}\varphi_{Sm} - \frac{\sin\alpha}{R}\varphi_{\theta m} + \frac{B_{66}}{\zeta_{10}} N_{S\theta m} - \frac{A_{66}}{\zeta_{10}} M_{S\theta m}$$

$$\frac{dN_{sm}}{ds} = \left(-I_0\omega^2 + \frac{\zeta_6 \sin^2\alpha}{R^2}\right) u_m + \frac{m\zeta_6 \sin\alpha}{R^2} v_m + \frac{\zeta_6 \sin\alpha\cos\alpha}{R^2} w_m + \left(-I_1\omega^2 + \frac{\zeta_7 \sin^2\alpha}{R^2}\right)\varphi_{sm} + \frac{m\zeta_7 \sin\alpha}{R^2}\varphi_{\theta m} - \frac{\sin\alpha}{R}(1+\zeta_4) N_{sm}$$

$$- \frac{\zeta_2 \sin\alpha}{R} M_{sm}$$

$$\frac{dN_{s\theta m}}{ds} = -\frac{m\zeta_6 \sin\alpha}{R^2} u_m + \left(-I_0\omega^2 + \frac{kA_{44}\cos^2\alpha}{R^2} + \frac{m^2\zeta_6}{R^2}\right) v_m + \frac{m\cos\alpha}{R^2}(kA_{33} + \zeta_6) w_m - \frac{m\zeta_4}{R} N_{sm} - \frac{2\sin\alpha}{R} N_{s\theta m} - \frac{m\zeta_2}{R} M_{sm}$$

$$\frac{dQ_{sm}}{ds} = \frac{\zeta_6 \sin\alpha\cos\alpha}{R^2} u_m + \frac{m\cos\alpha}{R^2}(kA_{44} + \zeta_6) v_m + \left(-I_0\omega^2 + \frac{m^2 kA_{44}}{R^2} + \frac{\zeta_6 \cos^2\alpha}{R^2}\right) w_m + \frac{\zeta_7 \sin\alpha\cos\alpha}{R^2}\varphi_{sm} + m\left(-\frac{kA_{44}}{R} + \frac{\zeta_7 \cos\alpha}{R^2}\right)\varphi_{\theta m}$$

$$- \frac{\zeta_4 \cos\alpha}{R} N_{sm} - \frac{\sin\alpha}{R} Q_{sm} - \frac{\zeta_2 \cos\alpha}{R} M_{sm}$$

$$\frac{dM_{Sm}}{ds} = \left(2\zeta_8 \sin^2\alpha - I_1\omega^2\right) u_m + 2m\zeta_8 \sin\alpha v_m + 2\zeta_8 \sin\alpha\cos\alpha w_m + \left(2\zeta_9 \sin^2\alpha - I_2\omega^2\right)\varphi_{sm} + 2m\zeta_9 \sin\alpha\varphi_{\theta m} - 2\zeta_5 \sin\alpha N_{Sm}$$

$$+ Q_{sm} - \left[2\sin\alpha\left(\zeta_3 + \frac{1}{R}\right)\right] M_{sm} - \frac{m}{R} M_{S\theta m}$$

$$\frac{dM_{S\theta m}}{ds} = m\zeta_8 \sin\alpha u_m + \left(m^2\zeta_8 - \frac{kA_{44}\cos\alpha}{R} - I_1\omega^2\right) v_m + \left(m\zeta_8 \cos\alpha - \frac{mkA_{44}}{R} - I_0\omega^2\right) w_m + + m\zeta_9 \sin\alpha\varphi_{sm} \qquad (9)$$

$$+ \left(m^2\zeta_9 + kA_{44} - I_2\omega^2\right)\varphi_{\theta m} - m\zeta_5 N_{Sm} - m\zeta_3 M_{sm} - \frac{2\sin\alpha}{R} M_{S\theta m}$$

where:

$$\zeta_1 = A_{11}D_{11} - B_{11}^2,$$
$$\zeta_2 = \left(A_{12}B_{11} - A_{11}B_{12}\right)/R\zeta_1,$$
$$\zeta_3 = \left(B_{11}B_{12} - A_{11}D_{12}\right)/R\zeta_1,$$
$$\zeta_4 = \left(B_{11}B_{12} - A_{12}D_{11}\right)/R\zeta_1,$$
$$\zeta_5 = \left(B_{11}D_{12} - B_{12}D_{11}\right)/R\zeta_1,$$
$$\zeta_6 = \left(A_{12}\zeta_4 + B_{12}\zeta_2 + A_{22}/R\right)/R$$
$$\zeta_7 = \left(A_{12}\zeta_5 + B_{12}\zeta_3 + B_{22}/R\right)/R, \quad \zeta_8 = \left(B_{12}\zeta_4 + D_{12}\zeta_2 + B_{22}/R\right)/R \qquad (10)$$
$$\zeta_9 = \left(B_{12}\zeta_5 + D_{12}\zeta_3 + D_{22}/R\right)/R, \quad \zeta_{10} = B_{66}^2 - A_{66}D_{66}$$

These expressions can be written in matrix form as:

$$\frac{d\mathrm{y}_m}{ds} = \mathrm{A}_m(\mathrm{s},\omega)\mathrm{y}_m \qquad \text{with } \boldsymbol{A}_m \text{ is a 10x10 matrix} \qquad (11)$$

2.3.2. Dynamic transfer matrixes of cylindrical shell and ring

In this stage, the dynamic transfer matrix $\boldsymbol{T}(\omega)_m$ will be evaluated. However, due to the numerical computing errors when dealing with bound values of the cone angle (0 and $\pi/2$), it is important to calculate separately two matrixes $\boldsymbol{A}_m{}^c(\alpha=0)$, and $\boldsymbol{A}_m{}^r(\alpha=\pi/2)$ corresponding to cylindrical shell and rings. Then the two different dynamic transfer matrixes ($\boldsymbol{T}_m{}^c$ and $\boldsymbol{T}_m{}^r$) will be computed from these $\boldsymbol{A}_m{}^c$ and $\boldsymbol{A}_m{}^r$ matrix. The method to construct the dynamic transfer matrix and then dynamic stiffness matrix from these $\boldsymbol{A}_m{}^c$ and $\boldsymbol{A}_m{}^r$ matrix is known and detailed in [13].

The dynamic transfer matrix $\boldsymbol{T}(\omega)_m{}^c$ for the cylindrical shell ($\alpha = 0$) can be evaluated as [14]:

$$T(\omega)_m^c = e^{\int_0^L A_m^c(\omega)ds} \tag{12}$$

with L the length of the cylindrical shell,

And the exponential matrix being given by [13]

$$e^X = \sum_0^\infty \frac{\boldsymbol{X}^k}{k!} \tag{12a}$$

The dynamic transfer matrix $\boldsymbol{T}(\omega)_m{}^r$ for the ring ($\alpha=\pi/2$) is computed by the following expression:

$$T(\omega)_m^r = e^{\int_0^{R_2-R_1} A_m^r(s,\omega)ds} \tag{13}$$

Here R_1 and R_2 are inner and outer radiuses of the rings.

2.3.3. Dynamic stiffness matrixes $\boldsymbol{K(\omega)_m}$ for cylindrical shell and ring

Despite of the different formulations to estimate the dynamic transfer matrix, the dynamic stiffness matrix $\boldsymbol{K}(\omega)_m$ will be obtained by the same procedure. Therefore, it is more convenient to use one matrix denoted $\boldsymbol{T}_m$ which may represent as $\boldsymbol{T}_m{}^c$ or $\boldsymbol{T}_m{}^r$ matrix depending on the studied cases. The following steps must be respected in order to build the matrix $\boldsymbol{K}(\omega)_m$: division of $\boldsymbol{T_m}$ and then construction of $\boldsymbol{K}(\omega)_m$.

First, the dynamic transfer matrix $\boldsymbol{T}_m$ can be divided into four blocks as:

$$\boldsymbol{T_m} = \begin{bmatrix} \boldsymbol{T}_{11} & \boldsymbol{T}_{12} \\ \boldsymbol{T}_{21} & \boldsymbol{T}_{22} \end{bmatrix} \tag{14}$$

Finally, the dynamic stiffness matrix $\boldsymbol{K}(\omega)_m$ for the cylindrical shell or the ring is determined as:

$$K(\omega)_{\boldsymbol{m}} = \begin{bmatrix} T_{12}^{-1}T_{11} & -T_{12}^{-1} \\ T_{21} - T_{22}T_{12}^{-1}T_{11} & T_{22}T_{12}^{-1} \end{bmatrix}_{\boldsymbol{m}} \tag{15}$$

2.3.4. Harmonic response and the detection of natural frequencies

As known, the Williams-Wittrick algorithm is usually considered to analyze the dynamic behavior of the structure at this stage. However, this approach required a large number of

mathematical operations resulting in a very low speed of computation. Therefore, our study exploited another efficient method widely used in experiment for measuring and testing vibrations of structures. This alternative consists of plotting the harmonic responses and then recognizing natural frequencies from those curves [13-16].

2.3.5. Dynamic stiffness matrix for thick composite ring-stiffened cylindrical shells

The proposed model demonstrates a major advantage compare with other approaches when dealing with structures having complex geometric configurations and material properties. The powerful and efficient assembling procedure of different single dynamic stiffness matrix allows a fast and accurate construction of the dynamic stiffness matrix for complicated structures. In this section, this special property of continuous element model will be exploited to analyze the vibrations of thick composite ring-stiffened cylindrical shells.

For studying those complex structures, analytical methods meet enormous difficulties to build and resolve huge differential equations of the system. In addition, the approximate Finite Element Method doesn't seem to be a precise and efficient way to deal with this problem due to the complicated and expensive operations to model and mesh structures with complex geometry and material properties, especially in medium and high frequency range.

Consider the composite cylindrical shells with one outer ring stiffener (see Fig. 1) in which the shell and ring may have different properties of thickness, dimensions and materials. For CE model, this complicated shell is divided into three continuous elements: one cylindrical shell element with length L_1, one ring element and another cylindrical shell element having the length L_2. These elements are represented by three dynamic stiffness matrix $\boldsymbol{K_1^c(\omega)}$, $\boldsymbol{K^r(\omega)}$ and $\boldsymbol{K_2^c(\omega)}$, respectively.

Following Kouchakzadeh and Shakouri [11] the continuity conditions at the connecting interface of cylindrical shell element 1, ring stiffener and cylindrical shell element 2 can be expressed as follows:

$$\begin{aligned}
&u_1 = -w_2 = u_3, w_1 = u_2 = w_3, v_1 = v_2 = v_3,\\
&\frac{\partial w_1}{\partial s_1} = \frac{\partial w_2}{\partial s_2} = \frac{\partial w_3}{\partial s_3}, N_{s1} = -Q_{s2} = N_{s3}, M_{s1} = M_{s2} = M_{s3}\\
&M_{s\theta 1} = M_{s\theta 2} = M_{s\theta 3} \qquad M_{s1} = M_{s2} = M_{s3}\\
&Q_{s1} + \frac{1}{R_1}\frac{\partial M_{s\theta 1}}{\partial \theta_1} = N_{s2} = Q_{s3} + \frac{1}{R_3}\frac{\partial M_{s\theta 3}}{\partial \theta_3}, \ \frac{M_{s\theta 1}}{R_1} + N_{s\theta 1} = N_{s\theta 2} = \frac{M_{s\theta 3}}{R_3} + N_{s\theta 3}
\end{aligned} \tag{16}$$

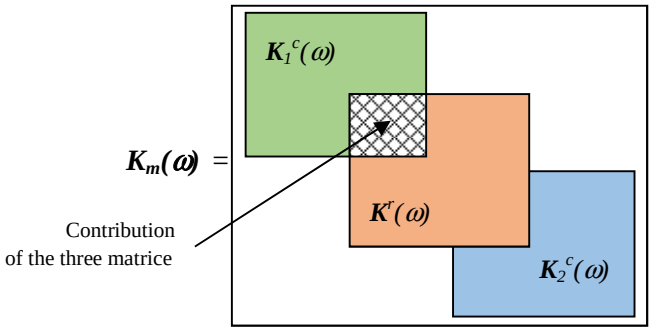

Figure 3. The assembling procedure to obtain the matrix $\boldsymbol{K_m(\omega)}$ for a ring-stiffened cylinder.

The association of these cylinders and ring-stiffener to form the whole structure corresponds to the assembly of the three above single dynamic stiffness matrix in order to obtain the dynamic stiffness matrix $\boldsymbol{K(\omega)}$ of the system. First, it is necessary to evaluate separately the dynamic stiffness matrix $\boldsymbol{K_1^c(\omega)}$, $\boldsymbol{K^r(\omega)}$ and $\boldsymbol{K_2^c(\omega)}$. Then the construction of the dynamic stiffness matrix $\boldsymbol{K(\omega)}$ for the ring-stiffened cylindrical shells based on the continuity conditions at the connecting is illustrated in Figure 3. Once $\boldsymbol{K(\omega)}$ is obtained, natural frequencies of ring-stiffened cylindrical shells will be extracted from harmonic responses [13-16].

3. NUMERICAL RESULTS AND DISCUSSIONS

First, the free vibration analysis of a ring-stiffened cylindrical shell have an external ring stiffener has been studied to confirm the precision of the proposed model. Obtained natural frequencies computed by CEM will be in comparison with analytical solutions of Wang and Lin [10]. Next, CE resolutions are compared with those of FEM and then harmonic responses will be presented and exploited to illustrate important advantages of CEM.

3.1. Modal analysis

To validate the precision of the presented formulations, numerical examples on free vibration analysis of clamped-clamped ring-stiffened cylindrical shells are conducted. Comparisons of natural frequencies are made with previously published results from Wang and Lin [10] using analytical method. The properties of the cylindrical shells and rings used for the analysis are listed in Table 1.

The cylindrical shells are made of composite material T300/976 Graphite/Epoxy with: E_1 = 150 GPa, $E_2 = E_3$ = 9 GPa, G_{23} = 2.5GPa, $G_{12} = G_{13}$ = 7.1GPa and υ_{12} = 0.3. It is interesting to remark that here the ring is made by another material. Here, the 6061-T6 aluminum is used for the ring with following characteristics: E_r = 70 GPa; G_r = 2.6 GPa, ρ_r = 2710 kg/m^3, and υ_r = 0.23. The calculated frequency is expressed in terms of a cycle frequency (rad/s).

Table 1. Geometrical and material properties of the ring-stiffened cylindrical shells.

Characteristics	**Geometrical and Material properties**
Number of rings N	1
Shell radius R (m)	0.3
Shell thickness h (m)	0.03
Shell length L (m)	5
Ring depth b_r (m)	0.01, 0.02, 0.03
Ring width c_r (m)	0.03, 0.06, 0.09
Stiffening type	External
Shell material	T300/976 Graphite/Epoxy
Ring material	6061-T6 aluminum

Tables from 2 to 4 show the comparison of our solutions in natural frequencies with those obtained by Wang and Lin [10] using an analytical method. Effects of width and thickness of the

stiffened ring and composite layer configurations on the modal frequencies of the structure are also examined.

Table 2. The thickness b effect of outer ring (c_r = 0.03m) on the comparison of the modal frequencies (rad/s) of the ring-stiffened $[90/0/90]_s$ laminated cylindrical shell ($L_1 = L_2$ = 2.5 m, R = 0.3 m, h = 0.03 m).

B	Mode	Frequency (rad/s)		
		Wang and Lin [10]	Present	Errors (%)
		A	B	=|(A-B)*100/A|
0.01	ω_{10}	3745.3	3704.6	1.08
	ω_{11}	723.1	718.2	0.67
	ω_{21}	1544.7	1533.1	0.75
	ω_{12}	2147.3	2126.9	0.95
	ω_{22}	2263.4	2231.2	1.42
0.02	ω_{10}	3731.6	3677.6	1.45
	ω_{11}	720.2	712.5	1.07
	ω_{21}	1549.2	1532.5	1.08
	ω_{12}	2161.9	2135.1	1.24
	ω_{22}	2268.7	2231.2	1.65
0.03	ω_{10}	3717.4	3663.1	1.46
	ω_{11}	717.2	709.4	1.09
	ω_{21}	1553.7	1532.4	1.37
	ω_{12}	2182.7	2135.1	2.18
	ω_{22}	2273.7	2231.2	1.87

Table 3. The width c_r effect of outer ring (b = 0.03 m) on the modal frequencies (rad/s) of the ring-stiffened $[90/0/90]_s$ laminated cylindrical shell ($L_1 = L_2$ = 2.5 m, R = 0.3 m, h = 0.03 m).

C	Mode	Frequency (rad/s)		
		Wang and Lin [10]	Present	Errors (%)
		A	B	=|(A-B)*100/A|
0.03	ω_{10}	3745.3	3704.6	1.08
	ω_{11}	723.1	718.2	0.67
	ω_{21}	1544.7	1533.1	0.75
	ω_{12}	2147.3	2126.9	0.95
	ω_{22}	2263.4	2231.2	1.42
0.06	ω_{10}	3676.5	3603.4	1.99
	$\omega 11$	708.6	697.5	1.57
	$\omega 21$	1565.3	1533.1	2.06
	$\omega 12$	2194.2	2164.6	1.35
	$\omega 22$	2283.1	2232.5	2.22
0.09	ω_{10}	3636.3	3546.3	2.48
	ω_{11}	700.3	685.5	2.11
	$\omega 21$	1575.2	1533.1	2.67
	$\omega 12$	2196.7	2170.9	1.17
	$\omega 22$	2288.8	2233.1	2.43

Table 4. The layers effect on the comparison of the modal frequencies (rad/s) of the laminated cylindrical shell ($L_1 = L_2 = 2.5$ m, $a = 0.3$ m, $h = 0.03$ m) with an outer stiffening ring ($b = 0.03$ m, $c_r = 0.06$ m).

Lamination Schemes	Mode	Frequency (rad/s)		
		Wang and Lin [10]	Present	Errors (%)
		A	B	=(A-B)*100/A
$[0/90/0]_s$	ω_{10}	4695.2	4885.8	4.06
	ω_{11}	787.1	776.6	1.33
	ω_{21}	1667.7	1648.1	1.18
	ω_{12}	1530.2	1512.4	1.16
	ω_{22}	1673.0	1629.9	2.58
$[90/0/90]_s$	ω_{10}	3676.5	3603.4	1.99
	ω_{11}	708.6	697.5	1.57
	ω_{21}	1565.3	1533.1	2.06
	ω_{12}	2194.2	2164.6	1.35
	ω_{22}	2283.1	2232.5	2.22

Table 2 demonstrates the modal frequencies of the $[90/0/90]_s$ laminated shell with an outer stiffening ring ($c_r = 0.03$ m) of three different thicknesses ($b = 0.01$ m, 0.02 m, 0.03 m) computed by CEM and by the study of Wang and Lin [10]. Furthermore, the comparisons of modal frequencies of the $[90/0/90]_s$ laminated shell with an outer stiffening ring $b_r = 0.03$ m of three different widths ($c_r = 0.03$ m, 0.06 m, 0.09 m) are considered in Table 3. At last, the comparisons of two different composite lamination schemes $[0/90/0]_s$ and $[90/0/90]_s$ on the modal frequencies of the composite joined ring-stiffened cylindrical shells with an outer stiffening ring $b = 0.03$ m, $c_r = 0.06$ m are indicated in Table 4.

It can be clearly seen in these tables that our solutions are in good agreements with results issued from [10] with various shells, ring-stiffeners and material parameters. Obtained errors between our model and those of Wang and Lin varying from 0.67 % to 4.06 % allow confirming that the proposed formulation is robust, exact and can be employed to study the dynamic behaviors of composite ring-stiffened cylindrical shells.

3.2. Vibration of composite ring-stiffened cylindrical shells

Now, the vibration of composite ring-stiffened cylindrical shells in which both shell and outer ring are made of the composite material will be examined.

Table 5. Geometrical and material properties of the composite joined ring-stiffened cylindrical shells.

Characteristics	**Geometrical and Material properties.**
Number of rings N	1
Shell radius R (m)	0.1
Shell thickness h (m)	0.002
Shell length L (m)	0.2
Ring depth b_r (m)	0.002
Ring width c_r (m)	0.01
Stiffening type	External
Shell and ring material	Graphite/Epoxy

Table 6. Comparison of natural frequencies (Hz) of composite ring- stiffened cylindrical shells with free-free and clamped- clamped boundary conditions.

BCs	Mode	Frequency (Hz)		
		CEM	FEM	Errors (%)
F-F	1.2	224	212	5.35
	2.2	355	345	2.81
	1.3	609	605	0.63
	2.3	850	855	0.61
	3.3	2589	2588	0.03
	1.4	1158	1157	0.06
	2.4	1373	1380	0.50
	3.4	2526	2544	0.71
	1.5	1858	1860	0.10
	2.5	1984	1988	0.20
	3,5	2855	2876	0.73
C-C	1.2	1845	1884	2.11
	2.2	3607	3767	4.43
	1.3	1690	1707	1.00
	2.3	2701	2872	3.73
	3.3	3985	3923	1.55
	1.4	2010	1961	2.43
	2.4	2381	2402	0.88
	3.4	3663	3767	2.83
	1.5	2497	2356	5.64
	2.5	2550	2420	5.09
	3.5	3857	3767	2.33

Table 5 summarizes information about the configurations of the studied structure and the composite material used for the investigation (Graphite/Epoxy) which have following characteristics: E_1 = 135GPa, $E_2 = E_3$ = 8.8GPa, $G_{12} = G_{13} = G_{23}$ = 4.47GPa, υ_{12} = 0.33 and the layer scheme is $[90/0]_2$. The same model has been constructed in FEM by using the Ansys software with the SHELL181 element for comparison. Results obtained by our formulation are compared with those of FEM in Table 6 for free-free (F-F) and clamped- clamped (C-C) boundary conditions. It can be observed that our results are in good agreements with finite element solutions. The maximum error is 5.35 % which confirms the reliability of the presented model.

3.3. The harmonic responses of composite ring-stiffened cylindrical shells

The harmonic response method was used to determine the natural frequencies of structures in previous studies (Casimir et al. [13, 14, 15], Cuong and Thinh [16]). In this section, the

harmonic responses of composite ring-stiffened cylindrical shells are in investigation in order to emphasize important advantages of the proposed model with common used approximate methods like the FEM. The dimensions and material properties of shells and ring are the same as those described in Table 5 and two kinds of boundary conditions: free- free (F-F) and clamped-free (C-F) are chosen for plotting the harmonic responses. The ring dimensions are: $b = c_r = 0.03$ m. A concentrated harmonic force $F = 1e^{i\omega t}$ N is applied at one free end of the structure as illustrated in Fig. 4 and the value of the displacement w will be extracted at the same point. The obtained displacements of this point will be used for constructing the harmonic response of the composite ring-stiffened cylindrical shell.

The CE harmonic response curve will be compared with those obtained with the finite element method using a raw meshing (35x25x3) and a fine meshing (65x50x3). Fig. 5 and Fig. 6 show harmonic responses of composite joined ring-stiffened cylindrical shell was calculated by CEM and by FEM for both free-free and clamped-free boundary conditions.

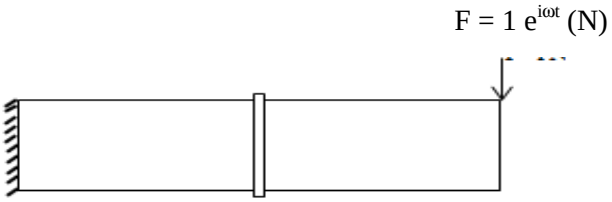

Figure 4. Geometry of composite joined ring-stiffened cylindrical shells used on harmonic responses with clamped- free boundary condition.

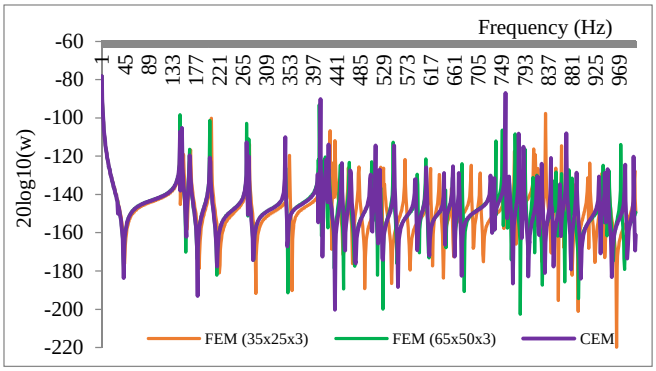

Figure 5. Comparison of harmonic responses of a free-free composite ring stiffened cylindrical shells obtained by CEM and by FEM.

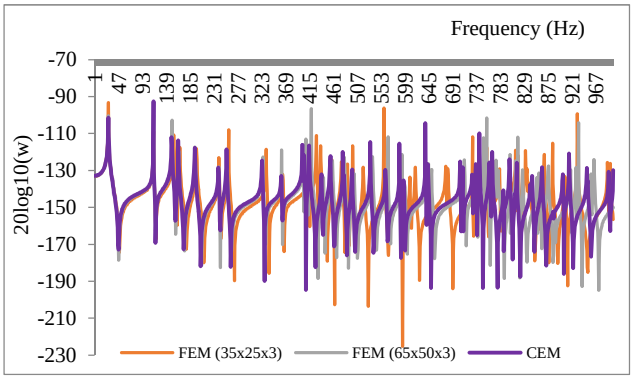

Figure 6. Comparison of harmonic responses of a clamped-free composite ring stiffened cylindrical shells obtained by CEM and by FEM.

It is easy to note seen that the solutions of CE model coincides to those of FEM in low frequencies since the three harmonic response curves are identical until 353 Hz for F-F boundary conditions and until 309 Hz for the C-F case. As known, FE model gives unreliable solutions in medium and high frequencies thus FE curves differ from CE one. The accuracy of FEM decreases for higher natural frequencies which is not the case for CE resolutions. It is very important to remark that FE solutions converge to CE results when using a finer meshing. This proves that the CEM using analytical solutions of the system of differential equations of the structure offers excellent results in medium and high frequency range which can overcome the difficulties of FEM in dynamic problems. Otherwise, it is easy to note that that the harmonic response drawn by FEM takes much more time than CEM because a finer meshing requires a bigger stiffness matrix and more time to resolve the finite element equations.

Through these graphics, it is concluded that the presented formulation offers an interesting way to deal with dynamic analysis of complex shell. The main advantages of CE models in terms of precision and the saving of data volume and of computing time even in medium and high frequencies are confirmed.

4. CONCLUSIONS AND DEVELOPMENTS

A new Dynamic Stiffness Matrix has been successfully established for thick cross-ply laminated composite ring-stiffened cylindrical shells. The interesting assembling procedure of continuous elements has been efficiently applicable to construct the dynamic stiffness matrix of the composite ring-stiffened cylinders with different properties of materials. The effect of ring depths, ring widths and lamination schemes on natural frequencies is envisaged by using Dynamic Stiffness Method and solutions obtained are validated with respect to other approaches. Excellent agreements issued from the comparison of natural frequencies computed by Continuous Element model and other methods confirm the exactness and the performance of our formulation. Moreover, the harmonic responses of composite ring- stiffened cylindrical shells are also examined in order to demonstrate many advantages of Continuous Element Method compared with Finite Element models. It can be seen that the advantages of the dynamic stiffness formulation are: accuracy, reduction of storage data volume, facility to model complex shell structures, time consumption decreased and those strong points are preserved even in medium and high frequency ranges.

The developed Continuous Element can easily be extended for analyzing thick cross-ply laminated composite joined ring- stiffened conical-cylindrical shells, complex shells on elastic foundation, and combined rings-stiffened cylindrical-conical shells in contact with fluid.

Acknowledgement. This research is funded by Hanoi University of Science and Technology under Grant number: **T2017-039.**

REFERENCES

1. Mikulas M. M., Mc Elman J. A. - On the free vibration of eccentrically stiffened cylindrical shells and plates, NASA, TN-D 3010, 1965.
2. Egle D. M., Sewall J. L. - Analysis of free vibration of orthogonally stiffened cylindrical shells with stiffeners treated as discrete elements, AIAA J **6** (3) (1968) 518–26.
3. Beskos D. E., Oates J. B. - Dynamic analysis of ring-stiffened circular cylindrical shells, Journal of Sound and Vibration **75** (1981) 1–15.
4. Najafi A. M., Warburton G. B. - Free vibration of ring-stiffened cylindrical shells, Journal of Sound and Vibration **13** (1970) 9-25
5. Mustafa B.A.J., Ali R. - An energy method for free vibration analysis of stiffened circular cylindrical shells, Computer and Structures **32** (2) (1989) 335–363.
6. Jafari A. A., Bagheri M. - Free vibration of rotating ring stiffened cylindrical shells with non-uniform stiffener distribution, Journal of Sound and Vibration **296** (2006) 353–376.
7. Qu Y., Chen Y., Long X., Hua H., Meng G. - Vibrational analysis of ring-stiffened conical–cylindrical-spherical shells based on a modified vibrational approach, International Journalist of Mechanical science **69** (2013) 72–84.
8. Kim Y. W. and Lee Y. S. - Transient analysis of ring- stiffened composite cylindrical with both edged clamped, Journal of Sound and Vibration **252**(1) (2002) 1-17.
9. Zhao X., Liew K. M., Ng. T. Y. - Vibration of rotating cross-ply laminated circular cylindrical shells with stringer and ring stiffeners, International Journal of Solids and Structures **39** (2002) 529–545. .
10. Wang R. T., Lin Z. X. - Vibration analysis of ring-stiffened cross-ply laminated cylindrical shells, Journal of Sound and Vibration **295** (2006) 964–987.
11. Kouchakzadeh M. A., Shakouri M. - Free vibration analysis of joined cross-ply laminated conical shells, International Journal of Mechanical Sciences **78** (2014) 118-125
12. Fazzolari F. A. - A refined dynamic stiffness element for free vibration analysis of cross-ply laminated composite cylindrical and spherical shallow shells, Composites Part B: Engineering **62** (2014) 143–58
13. Casimir J. B., Nguyen M. C., Tawfiq I. - Thick shells of revolution: Derivation of the dynamic stiffness matrix of continuous elements and application to a tested cylinder, Computers and Structures **85** (2007) 1845–1857.
14. Tounsi D, Casimir J. B, Abid A., Tawfiq I., Haddar M. -Dynamic stiffness formulation and response analysis of stiffened shells, Computers and Structures **132** (2014) 75–83.
15. Casimir J. B., Khadimallah M. A., Nguyen M. C. - Formulation of the dynamic stiffness of a cross-ply laminated circular cylindrical shell subjected to distributed loads, Computers and Structures **166** (2016) 42–50.

16. Thinh T. I., Nguyen M. C. - Dynamic stiffness matrix of continuous element for vibration of thick cross-ply laminated composite cylindrical shells, Composite Structures **98** (2013) 93–102.
17. Reddy J. N. - Mechanics of Laminated Composite Plates and Shells: Theory and Analysis, 2nd edn, CRC press, New York, 2003.